

Taxonomical study on a sample of land snails from Nanuque (Minas Gerais, Brazil), with descriptions of three new species

LUIZ RICARDO L. SIMONE & RODRIGO B. SALVADOR

Abstract

A sample of land snails was recently collected in a fragment of Atlantic rainforest, in the vicinities of the city of Nanuque (north of Minas Gerais state, Brazil), totaling 15 species. The following new species are herein described: *Leiostracus carnavalescus* n. sp. and *Rhinus botocudus* n. sp. (Bulimulidae), and *Obeliscus boitata* n. sp. (Subulinidae), the first two accompanied by anatomical descriptions. Moreover, the geographical ranges of some species are extended to Minas Gerais: *Auris bilabiata*, *Bahiensis* cf. *bahiensis*, *Cyclopomops moricandi*, *Dysopeas muibum*, *Helicina boettgeri*, *Helicina variabilis*, *Prohappia besckei*, and *Rectartemon piquetensis*. The discovery of new species in such a small forest fragment is a clear reminder of how little the Brazilian terrestrial snail fauna is known. It also points to the fact that these few remaining forest fragments may house many new and possibly endemic species and should, therefore, be properly preserved.

Key words: Atlantic Forest, Caenogastropoda, Gastropoda, Neritimorpha, Pulmonata, Stylommatophora.

Zusammenfassung

Fünfzehn Arten Landschnecken wurden im Mai 2012 in einem atlantischen Regenwald-Fragment in der Umgebung der Stadt Nanuque im Norden des Bundesstaates Minas Gerais in Brasilien gesammelt. Die folgenden drei neuen Arten werden beschrieben: *Leiostracus carnavalescus* n. sp. und *Rhinus botocudus* n. sp. aus der Familie Bulimulidae sowie *Obeliscus boitata* n. sp. aus der Familie Subulinidae. In den ersteren beiden Beschreibungen werden auch ausführliche anatomische Merkmale berücksichtigt. Die folgenden Arten werden zum ersten Mal für Minas Gerais nachgewiesen: *Auris bilabiata*, *Bahiensis* cf. *bahiensis*, *Cyclopomops moricandi*, *Dysopeas muibum*, *Helicina boettgeri*, *Helicina variabilis*, *Prohappia besckei* und *Rectartemon piquetensis*. Die Entdeckung der drei für die Wissenschaft neuen Arten in dem kleinen Waldfragment ist ein deutlicher Hinweis darauf, wie gering die Kenntnis der brasilianischen Landschneckenfauna ist, und wie wichtig der Schutz auch kleiner Waldreste wäre, die viele neue und möglicherweise endemische Arten enthalten könnten.

Contents

1	Introduction	9
2	Materials and methods	9
3	Systematics	12
4	Discussion	29
5	References	29

1 Introduction

The southeastern region of Brazil is historically the most explored (and exploited) in the country: its natural covering was fiercely degraded through the few centuries of the country's history. However, many new discoveries still wait in the remnants of Atlantic rainforest, especially regarding the scarcely studied terrestrial molluscan fauna. An expedition in May 2012 by shell collector JOSÉ COLTRO Jr. and his team to the previously unsampled region of Nanuque, in northern Minas Gerais state, recovered many land snails. Part of this material was donated to the collection of the Museu de Zoologia da Universidade de São Paulo (MZSP, São Paulo, Brazil) and is studied herein. As a testament to the incomplete knowledge of the Brazilian fauna, some of the animals recovered are new species. This paper presents formal descriptions of these taxa and

extends the geographical distributions of some other previously known species.

Acknowledgements

We are deeply grateful to JOSÉ COLTRO Jr. (Femorale) for providing the material studied here; to LARA GUIMARÃES (MZSP) for helping with SEM examination; to BARBARA M. TOMOTANI (Netherlands Institute of Ecology, Wageningen, The Netherlands), CARLO M. CUNHA (Academy of Natural Sciences of Philadelphia, USA) and DANIEL ABBATE (MZSP) for some of the photos used here (BMT: photos of *Leiostracus* from Mantena; CMC: photos of the living animals; DA: photos of *Helicina boettgeri* and *Bahiensis*).

2 Materials and methods

All the specimens collected are land snails, mainly stylommatophoran pulmonates, but two neritimorph species and one

caenogastropod are also present. Most species are only represented by dry shells, usually in a good state of preservation; only four were captured alive: *Helicina variabilis*, *Leiostracus perucidus*, *Leiostracus carnavalescus* n. sp. and *Rhinus botocudus* n. sp. All the animals were collected in the vicinities of the city of Nanuque (17°50'51"S 40°22'47"W, ~120 m of elevation; Fig. 1), in the north of Minas Gerais state, very close to the borders with the states of Bahia and Espírito Santo. The locality is a very small fragment of Atlantic rainforest (area estimated at ca. 0.15 km²), close to the Mucuri River, surrounded by tomato crops and thus highly subject to anthropic action and degradation.

The animals collected alive were preserved in 70% ethanol. Specimens were extracted from their shells and dissected (immersed in ethanol) by standard techniques under a stereomicroscope. Digital photographs were obtained for most dissection steps, as well as drawings with the aid of a camera lucida. Measurements were made with a digital caliper or with the Zeiss ZEN 2011 software. The radulae were mounted on stubs, coated with a gold-palladium alloy and examined by scanning electronic microscopy (SEM) in the Laboratório de Microscopia Elettronica of MZSP.

Identification was conducted based on the catalogue by SIMONE (2006), the original descriptions and additional material housed in the collection of the MZSP. Measurements were made

with a digital caliper or with the aid of the Zeiss Axiovision SE64 Rel 4.8 imaging software. All specimens are deposited in the malacological collection of the MZSP. The list of examined material can be found together with the descriptions of the new species and, for the other species, on Tab. 1. Interestingly, specimens of the new *Leiostracus* species were found in the MZSP collection (from the municipalities of Mantena, Minas Gerais state, and Pinheiros and Sooretama, Espírito Santo state; Fig. 1) and were also included in the analysis.

Abbreviations

Shell measurements

D	shell greatest width (diameter)
d	aperture width
H	shell height
h	aperture height
S	spire height (excluding aperture)
S'	spire height (excluding body whorl)

Anatomical characters

aa	anterior aorta
ac	albumen chamber
ad	albumen gland duct

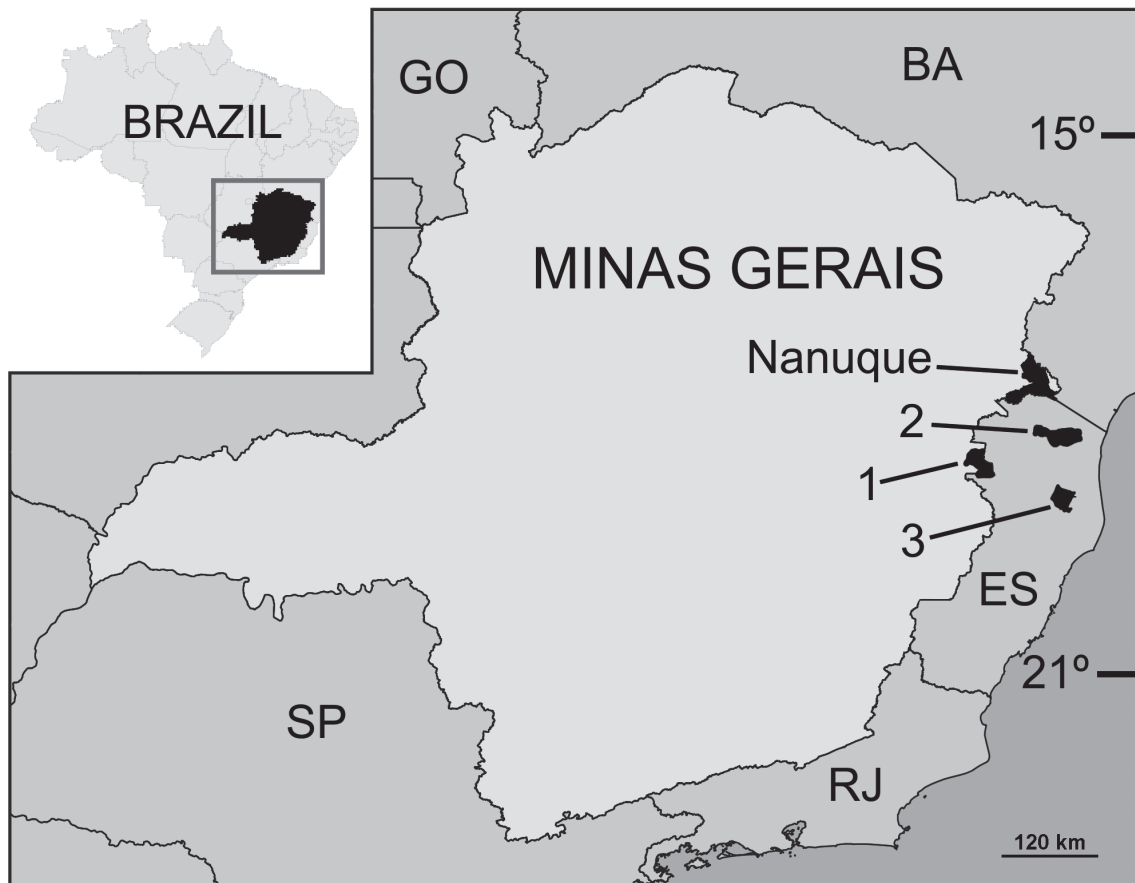


Fig. 1. Map showing the municipality of Nanuque, where the specimens studied here were collected, and the other municipalities from where the specimens of *Leiostracus carnavalescus* n. sp. come from: (1) Mantena; (2) Pinheiros; (3) Sooretama. – Abbreviations of the neighboring states: BA, Bahia; GO, Goiás; ES, Espírito Santo; RJ, Rio de Janeiro; SP, São Paulo.

Tab. 1. Other species occurring in the present material from Nanuque, accompanied by data on the material analyzed, mean measurements (of adult specimens) and previously known geographic distribution (sensu MORRETES 1949, SIMONE 2006). *Record from ROBINSON & SLAPCINSKY (2005). – Abbreviations: Material: sh., shell; spc., specimen. Brazilian states: BA, Bahia; CE, Ceará; ES, Espírito Santo; MG, Minas Gerais; PB, Paraíba; PE, Pernambuco; RJ, Rio de Janeiro; RN, Rio Grande do Norte; SC, Santa Catarina; SE, Sergipe; SP, São Paulo.

Species	Family	Material (MZSP)	Measurements	Distribution
<i>Auris bilabiata</i> (Broderip & Sowerby, 1829)	Bulimulidae	106155 (2 sh.)	H = 41.7, D = 27.3	Brazil (SE, BA, ES, RJ)
<i>Bulimulus tenuissimus</i> (d'Orbigny, 1835)	Bulimulidae	106158 (13 sh.)	H = 18.1, D = 9.2	USA (introduced*), Suriname, Brazil, Bolivia, Uruguay
<i>Leiostracus perlucidus</i> (Spix, 1827)	Bulimulidae	106160 (9 sh.), 106161 (1 spc.)	H = 22.3, D = 11.6	Guyana, Suriname, Brazil
<i>Helicina boettgeri</i> Wagner, 1910	Helicinidae	106166 (1 sh.), 106167 (6 sh.)	H = 3.1, D = 4.1	Brazil (ES)
<i>Helicina variabilis</i> Wagner, 1827	Helicinidae	106171 (1 spc.), 106172 (4 spc.), 106173 (1 sh.)	H = 9.7, D = 12.4	Brazil (PB, BA, ES, RJ)
<i>Cyclopomops moricandi</i> (Pfeiffer, 1852)	Megalomastomidae	106168 (1 sh.)	H = 3.4, D = 5.1	Brazil (BA)
<i>Bahiensis</i> cf. <i>bahiensis</i> (Moricand, 1833)	Odontostomidae	106165 (1 sh.)	H = 16.2, D = 5.1	Brazil (BA, RJ)
<i>Rectartemon piquetensis</i> (Pilsbry, 1930)	Streptaxidae	106156 (9 sh.)	H = 20.3, D = 31.6	Brazil (BA, SP)
<i>Megalobulimus bronni</i> (Pfeiffer, 1847)	Strophocheilidae	106154 (1 sh.)	H = 91.3, D = 56.0	Brazil (MG, ES, SP)
<i>Dysopeas muibum</i> Marcus & Marcus, 1968	Subulinidae	106163 (1 sh.)	H = 5.7, D = 2.4	Brazil (SP)
<i>Succinea meridionalis</i> d'Orbigny, 1837	Succineidae	106162 (1 sh.)	H = 8.2, D = 4.9	Brazil (RJ) to Argentina (Patagonia)
<i>Prohappia besckei</i> (Dunker in Pfeiffer, 1847)	Systrophiidae	106164 (6 sh.)	H = 4.4, D = 7.1	Brazil (RJ, SC), Paraguay

ag	albumen gland	gd	genital diverticulum
an	anus	gf	gastric inner fold
ap	genital aperture	go	gonad
au	auricle	hd	hermaphrodite duct
bc	bursa copulatrix	in	intestine
bd	bursa copulatrix duct	ir	insertion of m4 in subradular cartilage
bg	buccal ganglia	jw	jaw
bm	buccal mass	ki	kidney chamber
br	subradular membrane	kl	kidney lobe
ce	cerebral ganglion	m1–m13	extrinsic and intrinsic odontophore muscles
cm	columellar muscle	mb	mantle border
cn	cerebro-pedal and cerebro-pleural connectives	mf	mantle fold
co	collar vessel	mj	jaw and peribuccal muscles
cv	pulmonary (efferent) vein	mo	mouth
cy	statocyst	mu	ommatophore retractor muscle
da	digestive gland anterior lobe	mx	platform of mj in median line
dd	duct to digestive gland	ne	nephrostome
df	dorsal folds of buccal mass	nr	nerve ring
dg	digestive gland posterior lobe	oc	odontophore cartilage
di	diaphragm or pallial floor	od	odontophore
eh	epiphallus	of	odontophore cartilage median fusion with its pair
eo	spermoviduct	om	ommatophore
es	esophagus	pa	posterior aorta
ey	eye	pc	pericardium
fd	spermoviduct inner folds	pe	penis
ft	foot	pf	penis inner folds
ga	pedal gland aperture	pg	pedal gland

pi	penis inner chamber
pm	penis muscle
pn	pneumostome
pp	pedal ganglion
ps	penis sheath
pt	prostate
pu	pulmonary cavity
pv	pneumostome right flap
ra	radula
rn	radular nucleus
rs	radular sac
rt	rectum
sa	salivary gland aperture
sc	subradular cartilage
sd	salivary gland duct
sg	salivary gland
sp	sperm groove
sr	seminal receptacle
st	stomach
su	subesophageal ganglion
tg	integument
tm	tentacle retractor muscle
to	tissue on radular ribbon preceding radular exposed region in buccal cavity
ua	ureter aperture
ug	urinary gutter
un	union of mantle border with nuchal surface
up	primary ureter
ur	secondary ureter
ut	uterus
vd	vas deferens
ve	ventricle
vf	spermoviduct inner fold preceding vas deferens aperture
vg	vagina

3 Systematics

Gastropoda

Pulmonata

Stylommatophora

Family Bulimulidae

Genus *Leiostracus* Albers, 1850

Leiostracus carnavalescus n. sp.

(Figs. 2–27, 53–67)

Type material

Holotype: MZSP 106177 (Figs. 53–58).

Paratypes: MZSP 106178 (14 specimens), 106179 (24 shells), from type locality. J. COLTRO col., May/2012.

Type locality: Brazil. Minas Gerais: Nanuque, ~120 m of elevation (~17°51'S 40°23'W).

Additional material

Brazil. Minas Gerais: Mantena (city center coordinates: 18°46'55"S 40°58'48"W): MZSP 108010 (3 shells; ALEX B. BODART col., Feb/1993). – Espírito Santo: Pinheiros: Veado stream (“Córrego do Veado”): MZSP 106618 (4 specimens; FRANKLIN N. SANTOS col., 29/May/2011). – Sooretama: Contorno road (“Estrada do Contorno”): MZSP 106920 (1 specimen;

FRANKLIN N. SANTOS col., 14/Apr/2012). – Sooretama: Jequitibá trail (“Trilha do Jequitibá”): MZSP 106666 (1 specimen; FRANKLIN N. SANTOS col., 18/Jun/2012). – Sooretama: Quirininho trail (“Trilha do Quirininho”): MZSP 106650 (1 specimen; FRANKLIN N. SANTOS col., 14/Apr/2012).

Etymology

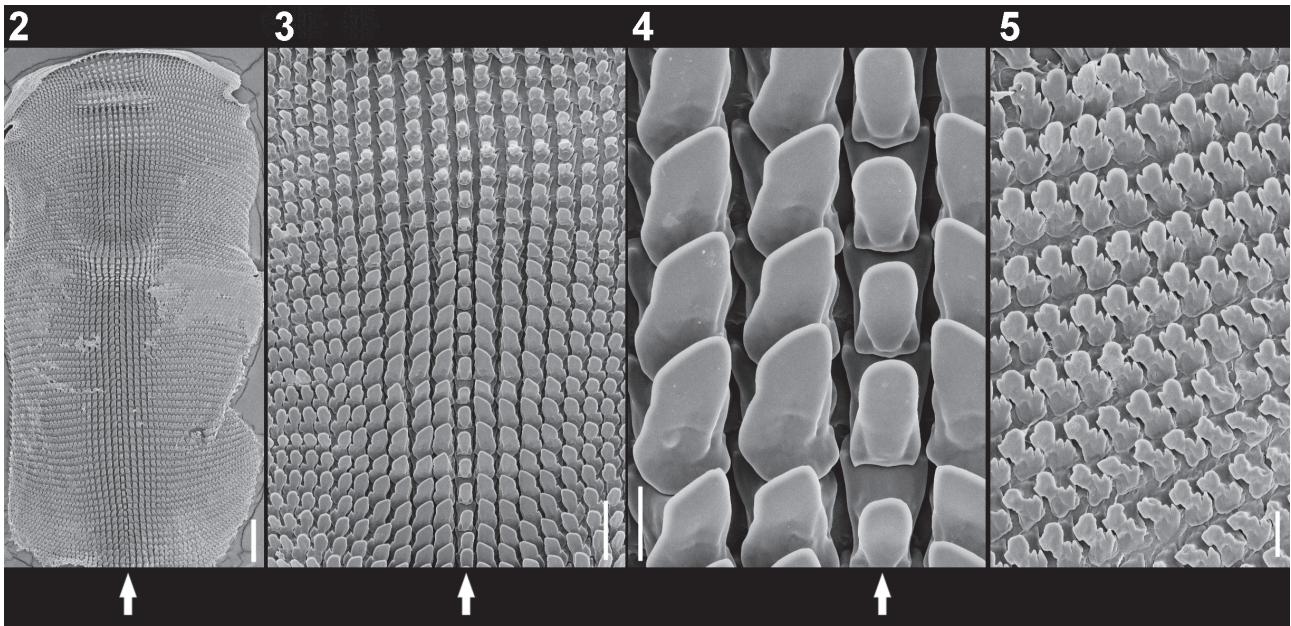
The name is a reference to the amazing variation in shell color in this species, establishing a parallel with the Carnival festival, when people dress in colorful costumes.

Diagnosis

Distinctive color pattern, with great intraspecific variation. Most usual color pattern is: spire top red, reddish orange or orange; spire with one broad spiral red or reddish brown band on middle portion of whorl, flanked by one or two lines of brownish dots; body whorl with dark brown or black spiral band on its base and red or light brown to dark brown spiral band close to the umbilicus.

Description

Shell (Figs. 53–65, 67): medium-sized (~25 mm), conical-oval; apex acuminate; greatest width on last whorl; width ~½ shell length. Base color white; color pattern with three main patterns (although some intraspecific variability can be found within these, mainly in color and thickness of the bands): (1) spire top red, reddish orange or orange; spire with one broad spiral red or reddish brown band on middle portion of whorl, flanked by one or two lines of brownish dots; body whorl with dark brown or black spiral band on its base and red or light brown to dark brown spiral band close to the umbilicus (Figs. 53–56, 59); (2) spire top orange; spire almost lacking white regions and with very thick orange spiral band on middle portion of whorl, flanked by lines of brownish dots; body whorl with many spiral bands below the orange one (from top to bottom: yellow band with the previously mentioned line of brownish dots superposed on it; dark brown or black band; another thick orange band; and, finally, a red band close to umbilicus) (Fig. 60); (3) spire top dark red to reddish brown; spire almost lacking white regions and with very thick spiral dark brown to black band and, below it, a single line of brownish dots; body whorl with greater white portion on its bottom, one dark brown or black spiral band on its base and another of same color close to umbilicus (Fig. 61). Spire angle ~40°. Protoconch of 1.5 whorl, sculptured by fine axial sinuous parallel riblets in upper portion and numerous fine spiral striae in lateral portion (Fig. 58); transition to teleoconch clear. Teleoconch smooth, except for growth lines. Whorl profile slightly convex. Suture well-marked. Aperture medium-sized, prosocline, oval; ~2/5 shell length, ~3/5 shell width. Peristome reflexed, especially on columellar region, partially covering umbilicus. Body whorl ~½ shell length. Umbilicus narrow.



Figs. 2–5. *Leiostracus carnavalescus* n. sp., SEM images of radulae. The arrows indicate the rachidian column. – 2. Whole view. 3. Detail of central region. 4. Greater detail of central region. 5. Detail of lateral region. – Scale bars: 20 μm (4), 50 μm (5), 100 μm (3), 300 μm (2).

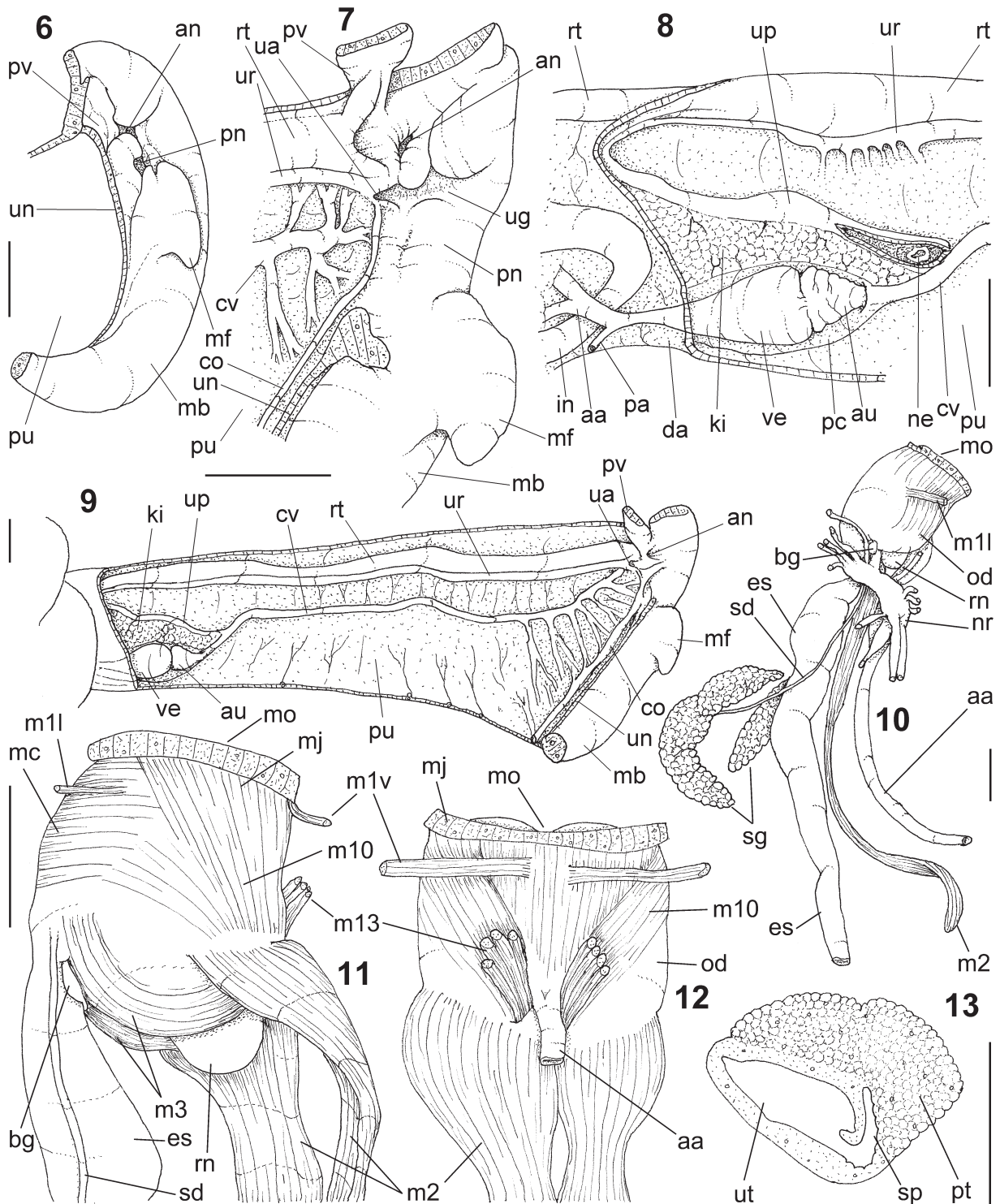
Head-foot (Figs. 14, 67): of normal shape. Color white, with a broad horizontal black band running continuously from frontal portion of head to middle portion of foot. Pair of ommatophores well-developed, with strong retractor muscles (tm). Eyes dark. Pair of tentacles brownish, with $\sim\frac{1}{2}$ ommatophores' length. Columellar muscle thick, 2 whorls in length, divided into 5–6 separated bundles (Fig. 14: cm); originating in lateral regions of haemocoel and running along its ventral surface; bundles connecting with each other in insertion region on the columella.

Mantle organs (Figs. 6–9): mantle border thick, lacking pigments. Pneumostome protected by ventral right flap (Figs. 6, 7: pv) with $\sim\frac{1}{4}$ of aperture length. Another similar-sized secondary fold is located on the left side of the pneumostome (Figs. 6, 7: mf). Pneumostome $\sim 10\%$ of aperture length, bearing exclusively the air entrance and the urinary gutter (Fig. 7: ua, ug); anus is a separated aperture located on the right of the pneumostome (Fig. 7: an). Lung of 1.5 whorls in length, narrow and elongated. Pulmonary vessels conspicuous only in anterior quarter (Fig. 9); remaining regions almost smooth, with imbricated vessels of difficult visualization (Fig. 9: pu). Pulmonary vein (Figs. 8, 9: cv) running longitudinally between middle and right thirds of pallial cavity roof. Kidney beige, located posteriorly, occupying $\sim 20\%$ of cavity length and $\sim 50\%$ of its width (details below). Rectum (rt) and ureter (ur) narrow, running along right edge.

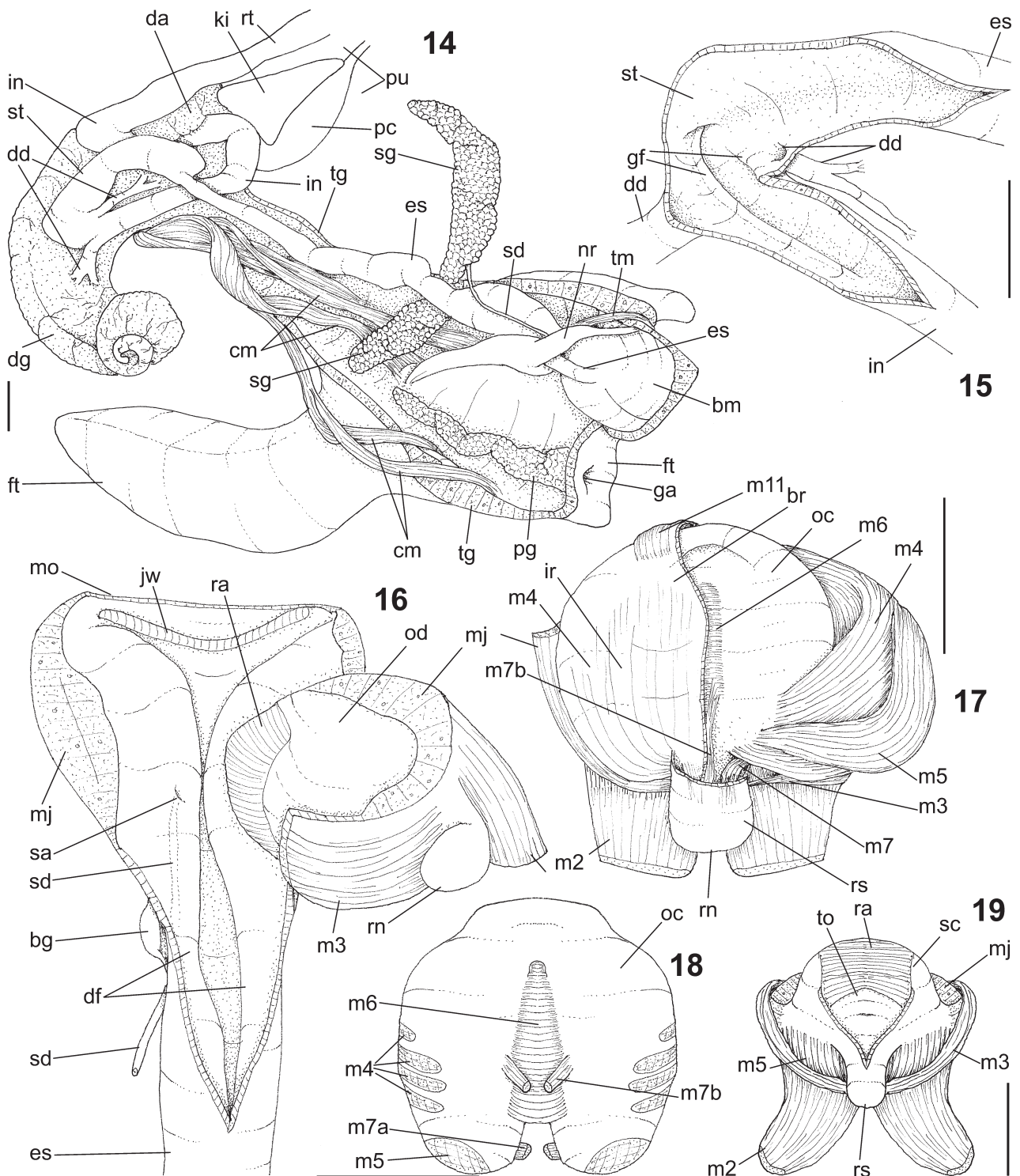
Visceral mass (Fig. 14): about 3.5 whorls in length. Both digestive gland lobes pale brown in color. Ante-

rior lobe (Fig. 14: da) flattened, occupying $\sim\frac{1}{6}$ of visceral volume, located just posteriorly to pallial cavity, continuous to kidney. Posterior lobe (dg) with 3 spiral whorls, occupying $\sim 70\%$ of visceral volume. Stomach occupying $\sim\frac{1}{8}$ of visceral volume, located between both digestive gland lobes, about half whorl posterior to pallial cavity (Fig. 14: st). Digestive tubes (described below) surrounding anterior lobe of digestive gland. Gonad clearly multi-lobed, cream colored, occupying entire second whorl, encased in middle-right region of posterior lobe of digestive gland, occupying $\sim\frac{1}{15}$ of visceral volume.

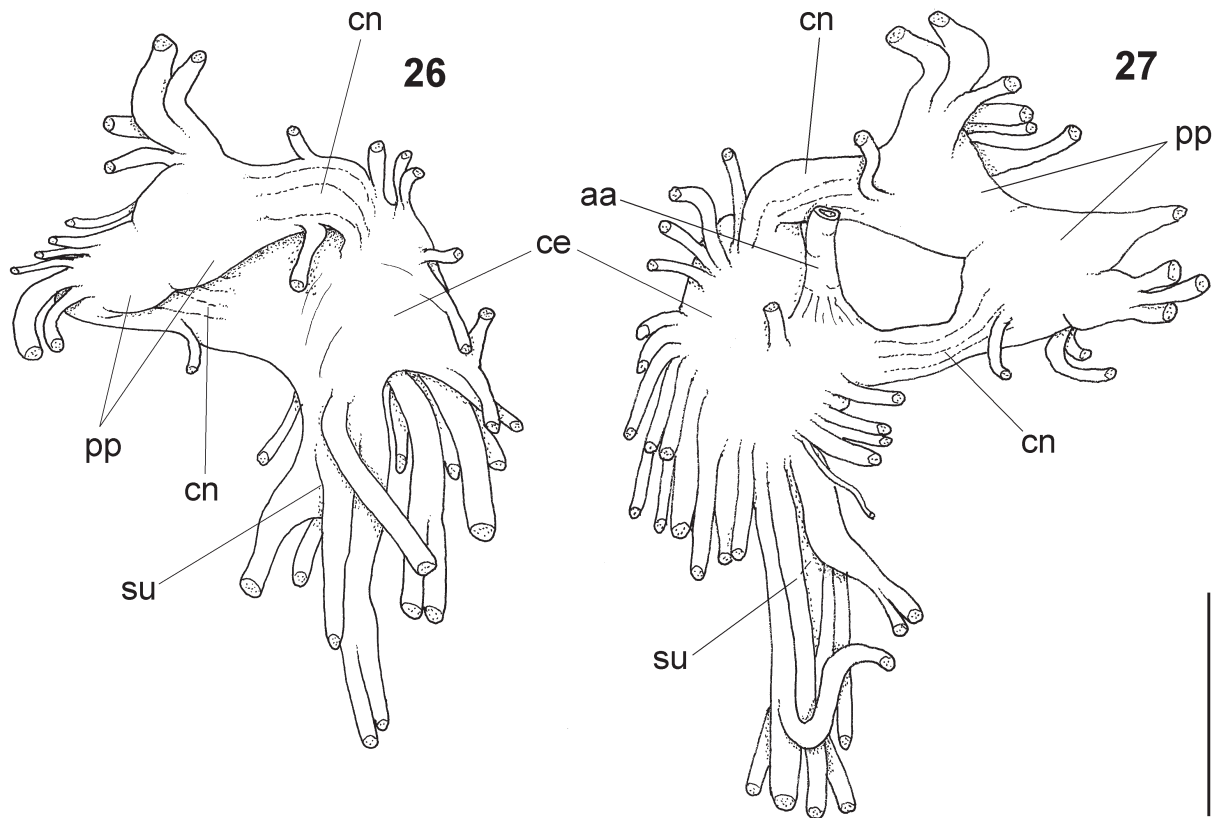
Circulatory and excretory systems (Figs. 8, 9): pericardium about twice as long as wide, located longitudinally between middle and left thirds of posterior end of pallial roof; occupying $\sim 5\%$ of lung area. Auricle (au) located anteriorly, as a continuation of the pulmonary vein; slightly smaller than the ventricle (ve). Kidney (ki) simple, entirely solid, dorsoventrally flattened; size reported above. Nephrostome small, located on anterior-left corner as the tip of a small projection of renal tissue, turned to the right (Fig. 8: ne). Primary and secondary ureter complete, closed (tubular); primary ureter lying on right edge of kidney, towards the posterior and right region, after forming a strong curve; afterwards running anteriorly, as secondary ureter (ur), along entire left edge of rectum. Urinary aperture (Fig. 7: ua) simple, turned anteriorly, located on right edge of pneumostome. Urinary gutter (Fig. 7: ug) running in front of urinary aperture, almost perpendicularly to mantle border, gradually disappearing.



Figs. 6–13. *Leiostracus carnavalescus* n. sp., anatomy. – 6. Detail of dorsal half of the mantle border, in frontal view. 7. Pneumostome region, in ventral view (ventral wall deflected upwards). 8. Reno-pericardial region, in ventral view (primary ureter opened longitudinally; the heart can be seen by transparency). 9. Pallial cavity, in inner ventral view (ventral edge of pneumostome deflected). 10. Foregut, in lateral (right) view (some of the more posterior structures were artificially separated from each other). 11. Buccal mass, in lateral (right) view. 12. Buccal mass, in ventral view. 13. Spermoviduct, transverse section in its middle region. – Scale bars: 1 mm (13), 2 mm (6–12).



Figs. 14–19. *Leiostracus carnavalescus* n. sp., anatomy. –14. Dissected specimen, largely in lateral (right) view (haemocoel opened longitudinally and deflected; visceral mass partially uncoiled; pallial cavity structures only partially shown; genital organs completely removed). 15. Stomach as seen in situ, in ventral view (ventral wall opened longitudinally). 16. Buccal mass, in ventral view (odontophore partially removed and deflected). 17. Odontophore, in dorsal view (the most superficial layer of muscles and membranes was removed; the left muscles were deflected to the right). 18. Odontophore's cartilages, in ventral view, showing the insertion marks of some muscles. 19. Odontophore, in dorsal view (radular sac partly opened longitudinally; m3 deflected downwards). – Scale bars: 2 mm.



Figs. 26–27. *Leiostracus carnavalescus* n. sp., anatomy. – 26. Central nervous system (nerve ring), in ventral view. 27. Central nervous system (nerve ring), in dorsal view. – Scale bar: 1 mm.

Digestive system (Figs. 10–12, 14–20): oral tube short, with thick muscular walls (Figs. 11, 12, 16: mj). Jaw simple; exposed portion horseshoe-shaped, bearing several uniform transverse folds (Figs. 16: jw, 66); color beige, translucent. Buccal mass spherical, $\sim 1/5$ of haemocoel volume (Fig. 14: bm). Dorsal surface of oral cavity with well-developed pair of dorsal folds (Fig. 16: df). Odontophore $\sim 3/5$ of buccal mass volume (Fig. 12: od). Odontophore muscles (Figs. 10–12, 16–20): mj, jaw and peribuccal muscle originating on outer-ventral surface of odontophore cartilages (Fig. 20: mj), running towards dorsal region, splaying on dorsal wall of oral tube (Figs. 16–17, 19: mj); m1, jugal muscles entirely covering haemocoelic structures, more concentrated close to the mouth; m1v, small pair of ventral retractor jugal muscles originating on lateral surface of haemocoel, close to the mouth, running towards medial region, inserting in ventral region of oral tube, close to the median line (Figs. 11, 12: m1v); m1l, small pair of lateral retractor jugal muscles originating on dorso-lateral region of haemocoel, on the same level as oral tube, running dorso-ventrally, inserting in latero-dorsal surface of oral tube (Figs. 10, 11: m1l); m2, strong pair of retractor muscles of buccal mass (or radular muscles) originating as one

pair of bundles of columellar muscle (Fig. 14: cm), running close to median line anteriorly along $\sim 80\%$ of haemocoel length, inserting as two different bundles in ventroposterior edge of odontophore, surrounding radular nucleus (Figs. 10, 16–17, 19–20: m2), passing through nerve ring (Fig. 10: nr); m3, transverse muscle of the posterior region of odontophore connecting both laterodorsal sides of odontophore, passing through odontophore posterior surface, in front of radular nucleus (Figs. 11, 16–17, 19: m3); m4, main pair of very thick dorsal tensor muscles of radula originating on posteromedial region of odontophore cartilages, in 3–4 oblique layers (Figs. 17–18: m4), surrounding the cartilages, inserting in subradular membrane (Fig. 17: ir); m5, pair of thick auxiliary dorsal tensor muscles originating on posteroventral region of odontophore cartilages (Fig. 18: m5), along $\sim 10\%$ of their length, running towards median line, inserting in subradular membrane by side of m4 insertion; m6, horizontal muscle thin, located between both cartilages in region just posterior to their fusion, along $\sim 2/5$ cartilages length, keeping free $\sim 1/6$ of cartilages length posterior to it (Figs. 17–18, 20: m6); m7, small pair of muscles originating in middle level of cartilages central edge, just posterior to m6 (Fig. 20: m7),

running medial-posteriorly inside radular sac, inserting splaying in dorsal posterior inner surface of radular sac (Fig. 17: m7); m7a, small pair of muscles of similar character as m7, but originating in posterior-medial corner of radular cartilages (Figs. 18, 20: m7a), running ventrally; m7b, small pair of narrow muscles originating in middle level of ventral edge of odontophore cartilages, covering m6, running posteriorly close to median line, inserting in dorsal inner surface of radular sac (Figs. 17–18: m7b); m11, pair of wide ventral tensor muscles of radula originating on ventrolateral surface of posterior region of cartilages (Fig. 20: m11), running close to the cartilages towards anterior region, inserting in ventral end of subradular membrane (br) (Fig. 17: m11); m13, pair of strong ventral odontophore protractor muscles originating on anteroventral region of haemocoel, running briefly towards dorsal region (Figs. 11, 12: m13), penetrating odontophore structures by lateral aorta insertion, inserting in outer-posterior surface of odontophore cartilages (Fig. 20: m13). Odontophore non-muscular structures (Figs. 17–20): oc, odontophore cartilages flattened, elliptical, circa three times longer than wide, fused with each other for $\sim 1/4$ of their anterior end (Figs. 18, 20: oc); anterior end roughly rounded; anterior region slightly curved medially; sc, subradular cartilage, with expanding region in buccal cavity protecting subradular membrane (Fig. 19: sc). Radular sac short, slightly extending beyond odontophore (Figs. 17, 19: rs).

Radula (Figs. 2–5) $\sim 50\%$ longer than odontophore; with rachidian teeth, and ~ 30 pairs of lateral teeth; no clear distinction between lateral and marginal teeth (Fig. 2). Rachidian tooth (Figs. 3–4: arrow) small, $\sim 1/70$ of radular width and roughly twice longer than wide; base wider, barely triangular; cutting edge slightly rounded, with $\sim 80\%$ of base length and 95% of base width. Lateral teeth similar to rachidian (Figs. 3–4), except in being slightly asymmetrical, weakly arched towards median region, and with cutting edge circa twice the size of rachidian's. Lateral teeth gradually decreasing towards lateral region; third or fourth teeth with gradually appearing basal-lateral cusp that becomes more and more distinct in more marginal teeth. Marginal teeth starts with no clear boundary with lateral teeth; shaped similarly to lateral teeth, except for being smaller and with a proportionally larger secondary cusp. There are more marginal teeth showing a bifid basal cusp (Fig. 5). Each radular row is disposed linearly on the same level (Fig. 2).

Salivary glands covering middle third of esophagus (Fig. 14: sg), forming two elongated white thin masses. Each salivary duct differentiable on anterior region of glands, with about 5–8% esophageal width. Salivary duct running on both sides of esophageal origin (Figs. 10, 14: sd), penetrating buccal mass wall on the region close to buccal ganglia (Fig. 16: sd). Salivary ducts opening on

anterior middle level of dorsal folds, slightly separated from median line (Fig. 16: sa).

Esophagus one whorl long, with thin flaccid walls lacking clear subdivisions (Figs. 10–11, 14: es); inner surface simple, smooth. Posterior esophageal half slightly narrower than anterior half. Stomach (Fig. 14: st) relatively narrow, curved, somewhat fusiform; position and size described above (visceral mass); gastric walls thin, flaccid; inner surface smooth (Fig. 15), except for narrow longitudinal fold (gf) from small gastric concavity up to intestinal origin, disappearing gradually. Esophageal insertion on right side, marked by sudden increase in size; intestinal origin on left side; both close to columella. Duct to anterior lobe of digestive gland encased between esophagus and intestine (Fig. 14: dd). Duct to posterior lobe of digestive gland located a short distance from intestinal origin and posteriorly to the above-described duct, directed towards the opposite side (Fig. 14: dd). Intestine as wide as esophageal insertion along its entire length, flanking the left side of the anterior lobe of digestive gland; on the region of the kidney, it gradually turns right and anteriorly, running almost straightly forward in the pallial cavity (Fig. 14: in). Rectum and anus described above (pallial cavity; Fig. 7).

Genital system (Figs. 21–25): gonad described above (visceral mass). Hermaphroditic duct (Fig. 11: hd) narrow and weakly coiled; running for $\sim 1/4$ whorl close to columella. Seminal receptacle (Figs. 22–23: sr) elongated, sac-like, strongly curved, with circa three times the hermaphroditic duct width, and $\sim 10\%$ its length. Fertilization complex simple, located on the base of seminal receptacle (Fig. 23) as a continuation of the hermaphroditic duct and the seminal receptacle's duct; $\sim 1/2$ width and length of receptacle. Fertilization complex totally immersed in albumen gland (Fig. 22), inserting in the posterior end of spermoviduct, in the albumen gland duct's region; all of them of similar width. Albumen gland (Figs. 21–23: ag) solid, white, elliptical, as large as gonad ($\sim 1/6$ whorl). Albumen gland duct subterminal, connected to distal end of spermoviduct, preceded by pair of large albumen chambers (Figs. 21–23: ac), each with $\sim 1/4$ albumen gland size, located on dorsal region of transition between albumen gland and spermoviduct, successively connected to the beginning of spermoviduct (Fig. 23). Spermoviduct ~ 1.5 whorl in length, slightly narrower than albumen gland, ~ 20 times longer than wide. Prostate gland occupying $\sim 1/2$ of the spermoviduct volume (Fig. 23: pt). Uterus occupying the other half of spermoviduct volume; external walls thick-glandular (Fig. 23: ut); inner surface completely covered by ample transversal folds (Fig. 25: ut); posterior diverticulum well-developed on the region immediately anterior to the albumen chambers (Fig. 23: gd). Sperm grove simple in posterior two thirds of spermoviduct (Fig. 13: sp), protected ventrally by a tall fold; gradually becoming tubular fold (Fig. 25: fd) as

vas deferens, along anterior third of spermoviduct, with $\sim 1/5$ of anterior spermoviduct width; bearing clear swelling (Fig. 25: vf) on region preceding exteriorization of vas deferens (Figs. 21, 25: vd). Vagina $\sim 1/10$ of spermoviduct length; inner surface simple, with 4–5 longitudinal, low, wide folds (Fig. 25: vg). Bursa copulatrix as long as spermoviduct plus albumen gland; bursa duct as wide as adjacent spermoviduct on its origin but gradually narrowing towards posterior end (Figs. 21, 25: bd); bursa elliptical, $\sim 1/3$ of albumen gland size (Fig. 21: bc), located encased between pericardium and adjacent intestinal loop. Penis $\sim 4/5$ of spermoviduct length, $\sim 2/3$ its anterior width (Fig. 21: pe); penis muscle inserting terminally, very short (Fig. 21: pm). No epiphallus. Vas deferens inserted subterminally in penis tip (Figs. 21, 24: vd). Internal penial surface with 3 clear sub-chambers (Fig. 24): posterior sub-chamber with $\sim 1/2$ penis length, bearing 4–5 longitudinal narrow low well-separated folds, some of them converging to the vas deferens aperture (vd), anterior quarter with fold becoming oblique and interrupted (pf); middle sub-chamber (pi) separated from other sub-chambers by transverse constrictions (posterior constriction slightly taller than anterior one), with $\sim 1/4$ penis length, internal surface bearing 10–12 longitudinal narrow closely-packed folds; anterior sub-chamber narrow, with $\sim 1/4$ of penis length, bearing 10–12 inner longitudinal low closely-packed folds. Penis shield with same length as anterior penial sub-chamber (Fig. 24: ps). Genital pore round, simple.

Central nervous system (Figs. 26–27): located dorsally from ventral base of buccal mass up to the transition between buccal mass and esophagus (Figs. 10, 14: nr). Pair of cerebral ganglia (ce) largely fused with each other; cerebral commissure invisible; each ganglion about as wide as adjacent esophageal section; several wide nerves originating on cerebral anterior edge, including relatively narrow subesophageal ganglion (su) located close to cerebral ganglia (but not fused with it). Pair of optical ganglia not individualized, possibly part of other nerves. Four parallel connectives (cn) between cerebral ganglia and pedal ganglia. Pair of pedal ganglia (pp) forming a single mass located opposite to the cerebral ganglia, slightly smaller in size than the latter. No differentiable ganglion detectable except for medial weak constriction. Several pairs of pedal nerves originating from latero-anterior corner of these ganglia. Anterior aorta (aa) clearly inserted in anteroventral region between both cerebral ganglia. Pair of statocysts not seen.

Measurements (in mm). Holotype: 8 whorls; H = 25.4; D = 12.4; S = 16.9; S' = 13.4; h = 9.2; d = 8.1. Mean (n = 17): 7 to 8 whorls; H = 24.4 ± 1.3 (max 26.6; min 22.8); D = 13.1 ± 0.9 (max 16.0; min 12.1); S = 14.9 ± 0.9 (max 16.9; min 13.6); S' = 11.7 ± 0.9 (max 13.4; min 10.4); h = 10.0 ± 0.8 (max 12.1; min 8.9); d = 7.6 ± 0.4 (max 8.3; min 6.9).

Distribution

Brazil. Minas Gerais: Nanuque (type locality) and Mantena municipalities. Espírito Santo: Pinheiros and Sooretama municipalities.

Habitat

Found on trees or tall bushes in Nanuque. Specimens from Mantena were found on subshrubs; specimens from Espírito Santo state have no habitat data. It is unknown whether its remarkable color pattern is related to camouflage, aposematism, or if it indeed plays some role on the animal's life at all. Still, it should be noticed that many specimens show signs of predation by birds.

Remarks

Leiostracus carnavalescus n. sp. bears some resemblance to *L. obliquus* (Reeve, 1849), from Bahia and Minas Gerais states (SIMONE 2006); however, it has a much thinner shell, a much less reflected peristome, wider and more conical shell, and the remarkable and variable color pattern (see description above). Shells with variable color pattern are not uncommon in the genus, but usually comprise only varying tones of yellow and brown (e. g., SIMONE 2006, SALVADOR & CAVALLARI 2013). The species which more closely resembles the pattern of *L. carnavalescus* is *L. vittatus* (Spix, 1827): it is white with one to three spiral brownish bands and some specimens show an “inverted” color pattern (base color brown with white spiral bands); moreover, it occurs in the states of Pernambuco and Bahia (SIMONE 2006), a neighboring distribution in relation to *L. carnavalescus*. Still, *L. carnavalescus* can be easily distinguished by its wider and more conical shell, with a smaller and rounder aperture.

The specimens from the municipality of Mantena (Fig. 1), approximately 130 km to the south of Nanuque, seem to belong to the same species as far as the conchological characters indicate. However, slight differences in coloration are evident (Figs. 64–65), although their importance cannot be evaluated without additional material. The specimens from Mantena are white with only two spiral bands on the body whorl (one red and the other, close to the umbilicus, dark brown), have an yellowish brown spire top and have only a single line of yellowish brown dots on their spire (these dots can be very large in some instances: Fig. 64). Moreover, in one specimen (Fig. 64), the suture line is marked with a brown line. Finally, while the animals from Nanuque were found on trees or tall bushes, the ones from Mantena were supposedly found on subshrubs, at least according to the specimens' labels.

The specimens from Espírito Santo state (Figs. 62–63), on the other hand, present a color pattern extremely similar to the type material from Nanuque; the single exception is that these specimens lack the spiral line of dots, having

a solid line instead. The municipality of Pinheiros is circa 65 km to the southeast of Nanuque, while the municipality of Sooretama is circa 150 km to the southeast (Fig. 1). Unfortunately, these specimens have no habitat data.

Anatomically, *L. carnavalescus* has the normal pattern of the Bulimulinae (BREURE & SCHOUTEN 1985; SIMONE 1998). The more remarkable features are the multiplicity of the columellar muscle bundles (Fig. 14: cm); the enlargement of the pedal gland (Fig. 14: pg); the multiplicity of the pair of odontophore muscles m7 (inside radular sac: m7, m7a, m7b; Figs. 17–18, 20); the pair of ventral protractor muscles of odontophore (Figs. 11, 12: m13); the two albumen chambers (Fig. 22: ac); the simplicity of the fertilization chamber (Fig. 23); and the penis divided into 3 sub-chambers (Fig. 24). The significance of these differences, in species, genus and family levels, is still under analysis.

Genus *Rhinus* Martens in Albers, 1860

Rhinus botocodus n. sp.
(Figs. 28–52, 68–76)

Type material

Holotype: MZSP 106174 (Figs. 68–73).

Paratypes: MZSP 106175 (2 specimens), 106176 (10 shells), from type locality. J. COLTRO col., May/2012.

Type locality: Brazil. Minas Gerais; Nanuque, ~120 m of elevation (~17°51'S 40°23'W).

Etymology

Reference to the “Botocudos” native Indians who once dwelt in the region.

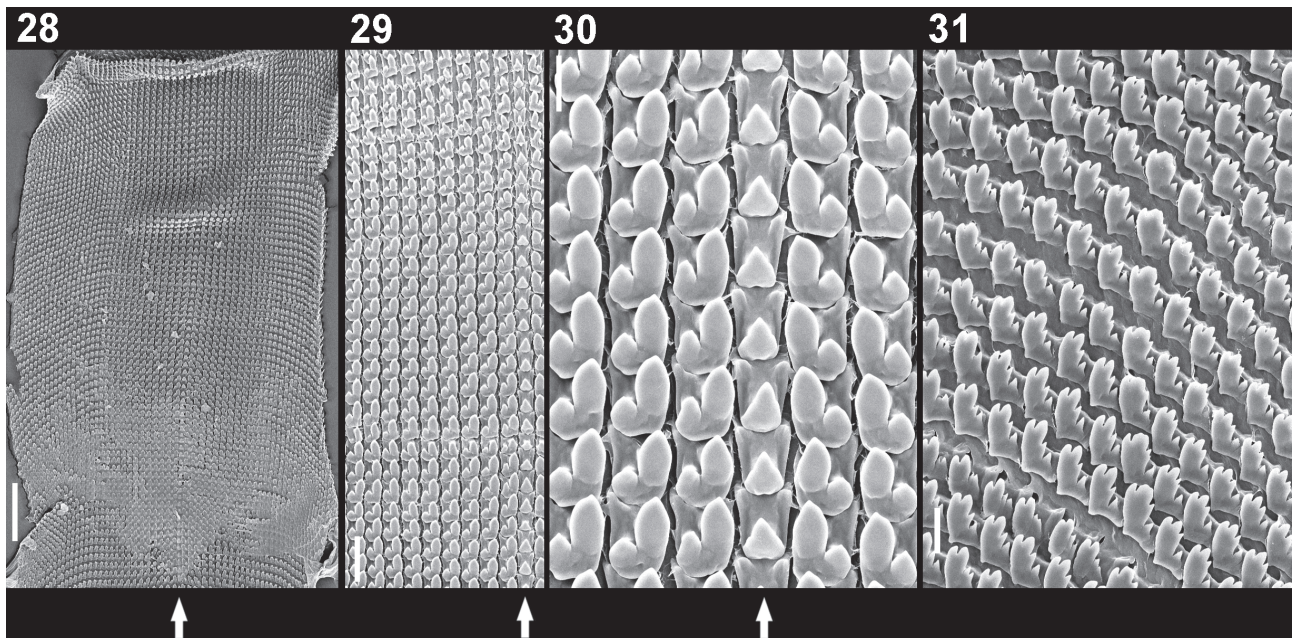
Diagnosis

Shell small and globose; aperture large and elongated diagonally. Protoconch with different sculpture patterns on upper and lateral portions of the whorl. Whitish spiral line running on the middle portion of body whorl.

Description

Shell (Figs. 68–74): medium-sized, ovoid to globose; diameter $\sim\frac{3}{4}$ shell length. Color yellowish brown to light brown, with whitish spiral line on middle portion of body whorl (Fig. 68). Spire angle $\sim 75^\circ$. Protoconch of 1.5 whorl, sculptured by axial parallel riblets on upper portion of whorl and spiral parallel striae on lateral portion of whorl (Fig. 72); transition to teleoconch clear, orthocline. Teleoconch smooth, except for growth lines, with lightly hairy periostracum; hairs arranged in spiral parallel lines, ~ 45 on body whorl, uniformly spaced and distributed (Fig. 73). Whorl profile convex. Suture well-marked. Aperture large, oval, diagonally elongated, slightly prosocline; $\sim\frac{3}{5}$ shell length, $\sim\frac{2}{3}$ shell width. Peristome slightly reflexed, more reflexed on columellar region, partially covering umbilicus. Body whorl $\sim\frac{3}{4}$ shell length. Umbilicus narrow.

Head-foot (Figs. 37, 38, 74): features similar to *Leiostracus carnavalescus* (see above), with the following



Figs. 28–31. *Rhinus botocodus* n. sp., SEM images of radulae. The arrows indicate the rachidian column. – 28. Whole view. 29. Detail of central region. 30. Greater detail of central region. 31. Detail of marginal region. – Scale bars: 20 μm (30, 31), 50 μm (29), 200 μm (28).

differences: Color uniformly dark grey on exposed areas (Fig. 74). Pair of ommatophores retractor muscles elongated, originating from columellar muscle (Fig. 37: mu). Columellar muscle of 1.5 whorl in length, divided into 4–5 separated bundles (Figs. 37–38: cm).

Mantle organs (Figs. 32–35): features similar to *Leiostracus carnavalescus* (see above), with the following differences: Mantle border thick and very tall (Fig. 32: mb). Secondary fold of mantle border located on bottom side of mantle collar (Figs. 32–33: mf). Outer pneumostome fold with circa twice the length of inner fold. Anus is a separated aperture located to the right of the pneumostome (Figs. 32, 34: an). Lung relatively wide. Anterior three quarters of pulmonary vessels conspicuous (Fig. 32); posterior quarter nearly smooth; venation absent on the region close to pneumostome (Fig. 34). Kidney occupying ~30% of cavity length and ~50% of its width.

Visceral mass (Fig. 39): features similar to *Leiostracus carnavalescus* (see above), with the following differences: Visceral mass ~2.5 whorls in length; stomach ~1/6 of visceral volume (Fig. 39: st).

Circulatory and excretory systems (Figs. 32–35): features similar to *Leiostracus carnavalescus* (see above), with the following differences: Pericardium occupying ~10% of lung area. Kidney with coiled kidney lobe (“roulade-like”; Fig. 36: kl). Nephropore punctiform, located on anterior-left corner (Fig. 35: ne). Urinary aperture wide (Fig. 32: ua). Urinary gutter well-delimited by pair of folds, running parallel to mantle border (Fig. 34: ug).

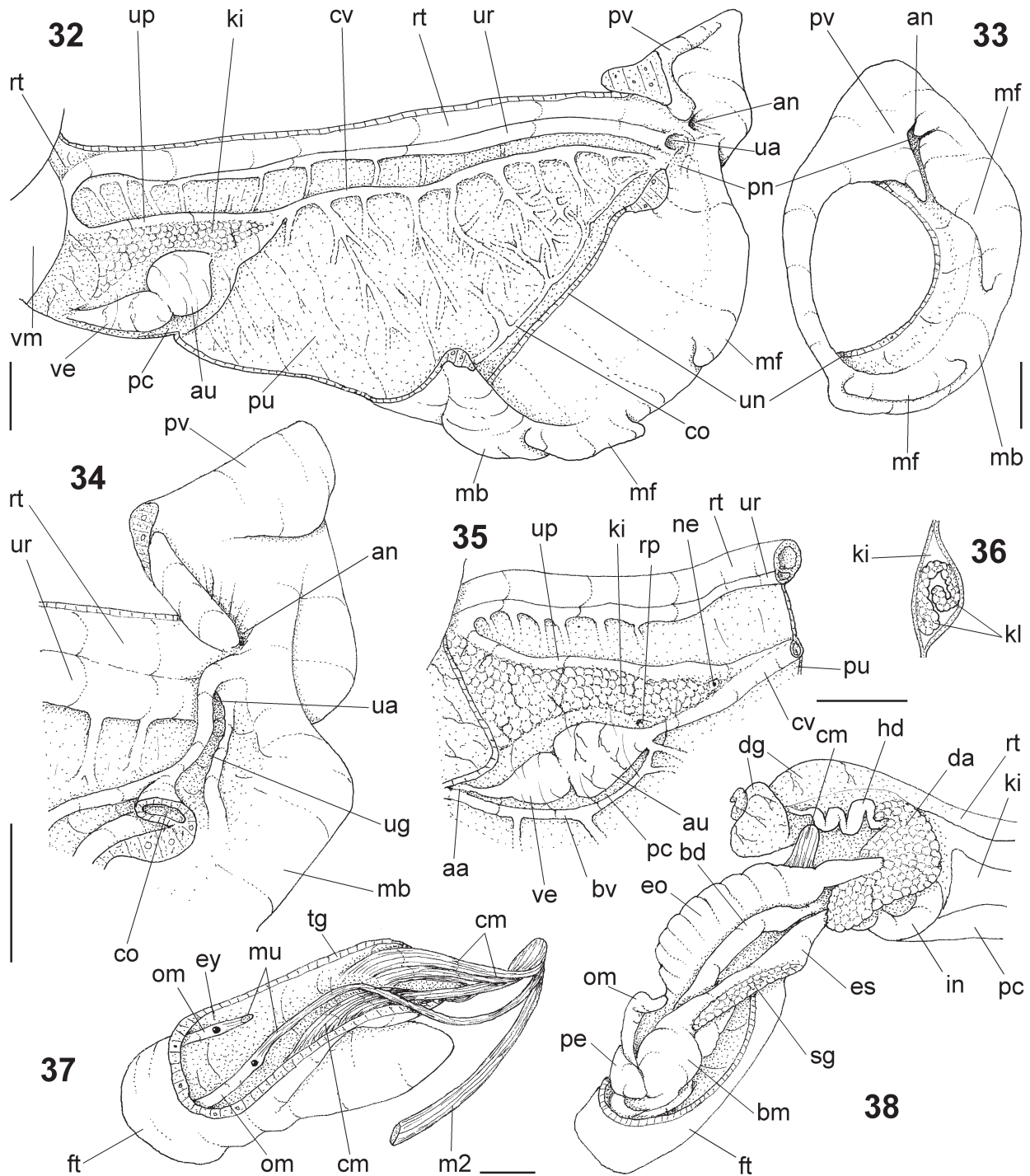
Digestive system (Figs. 38–45): features similar to *Leiostracus carnavalescus* (see above), with the following differences: Jaw with constant width along its length, bearing fewer transverse folds; median folds more perpendicular to edges (Figs. 40: jw, 75–76); color yellow, translucent. Buccal mass occupying ~1/6 of haemocoel volume (Fig. 38: bm). Pair of dorsal folds or oral cavity slightly narrower (Fig. 40: df). Salivary apertures (sa) located slightly more posteriorly. Differences in odontophore muscles (Figs. 40–45): mj, origin more elongated and posteriorly located (Fig. 45: mj); m1v and m1l pairs undetectable; m1d, pair of small dorsal protractor muscles (Fig. 41: m1d) originating on dorsal peribuccal inner surface of haemocoel, running to posterior region flanking buccal mass and inserting in posterior-dorsal surface of buccal mass; m2, slightly narrower near insertion (Figs. 42–43: m2), inserting in m4 instead of cartilages; m3, narrower (Fig. 40: m3); m3p, pair of thin and narrow muscles with dorsoventral fibers connecting lateral region of esophageal origin with ventral region of m2 insertion (Figs. 40–41: m3p); m4, slightly thicker (Figs. 42–43: m4); m5, shorter and thinner (Fig. 43: m5); m6, narrower on posterior region (Figs. 43, 45: m6); m7, m7a and m7b undetectable; m11, originating more anteriorly, narrower near origin (Fig. 45: m11); m13, slightly thicker near origin (Fig. 45: m13), but quickly nar-

rowing (Figs. 41–42: m13); mx, strong thick muscular layer produced medially by mj pair, passing posteriorly to both odontophore cartilages (Fig. 42: mx). Differences in odontophore’s non-muscular structures (Figs. 42–45): odontophore cartilages’ anterior junction slightly more pointed (Fig. 43: oc), fused with each other along ~1/5 of their length, on their anterior end (Figs. 44–45: of).

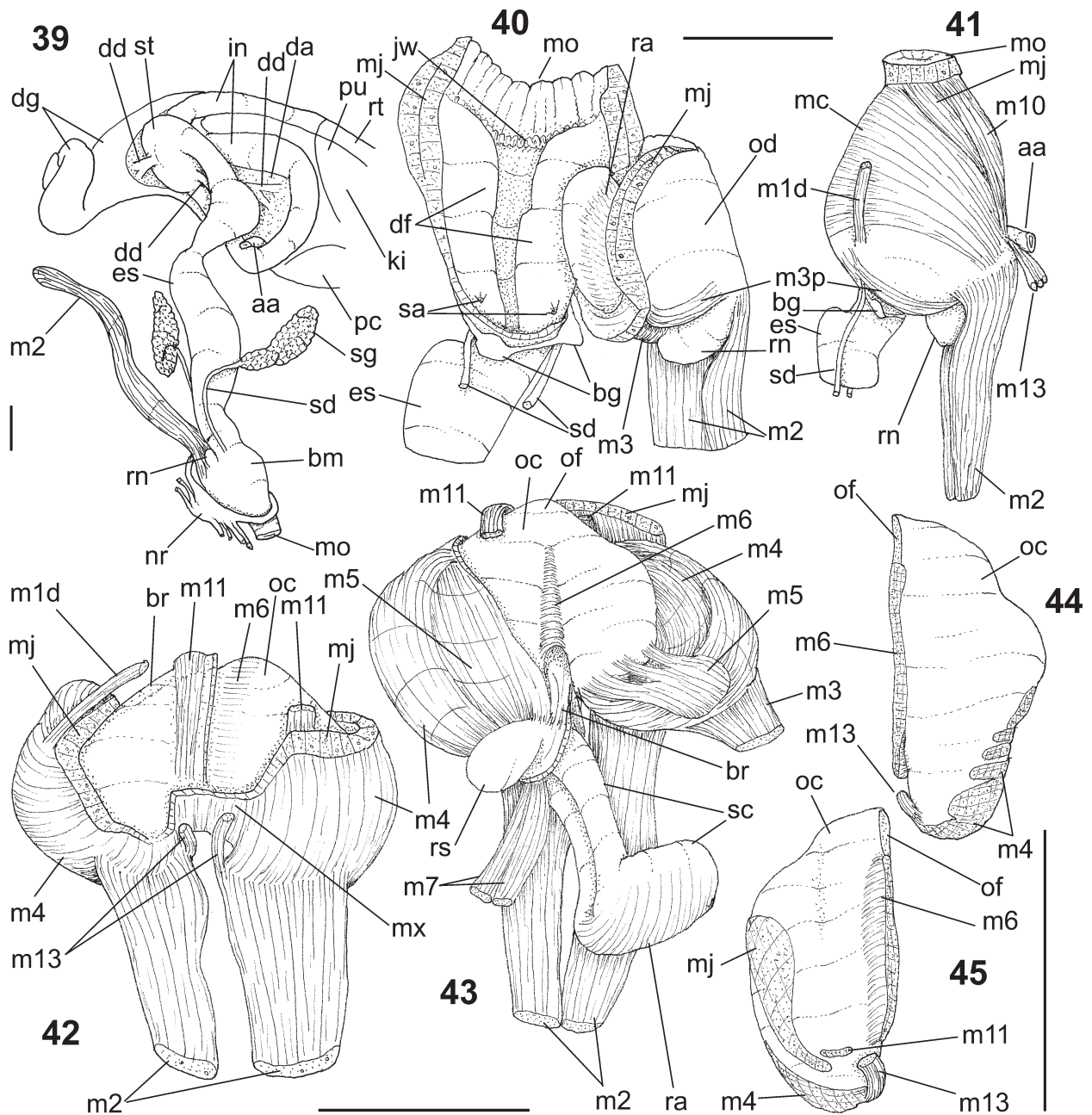
Differences in radula (Figs. 28–31): ~40 pairs of lateral teeth; distinction between lateral and marginal teeth somewhat clear, marked by abrupt inclination of tooth row (Fig. 28). Rachidian tooth (Figs. 29–30: arrow) ~1/80 of radular width and circa twice longer than wide; base with circa twice the length of cutting edge; cutting edge somewhat triangular, pointed. Lateral teeth (Figs. 29–30) always with secondary lateral cusp (of ~1/2 main medial cusp size); ~10 pairs of lateral teeth per row. Marginal teeth with 2–3 small secondary cusps on main cusp; basal cusp small, slightly bifid (Fig. 31).

Esophagus lacking clear subdivisions along its length (Fig. 39: es); lacking duct to anterior lobe of digestive gland. Stomach (Fig. 39: st) spherical; gastric walls thin; inner surface bearing uniform cover of narrow longitudinal folds. Duct to anterior lobe of digestive gland encased between esophagus and intestine, opening directly into anterior region of stomach (Fig. 39: dd). Duct to posterior region located on the middle of posterior gastric surface.

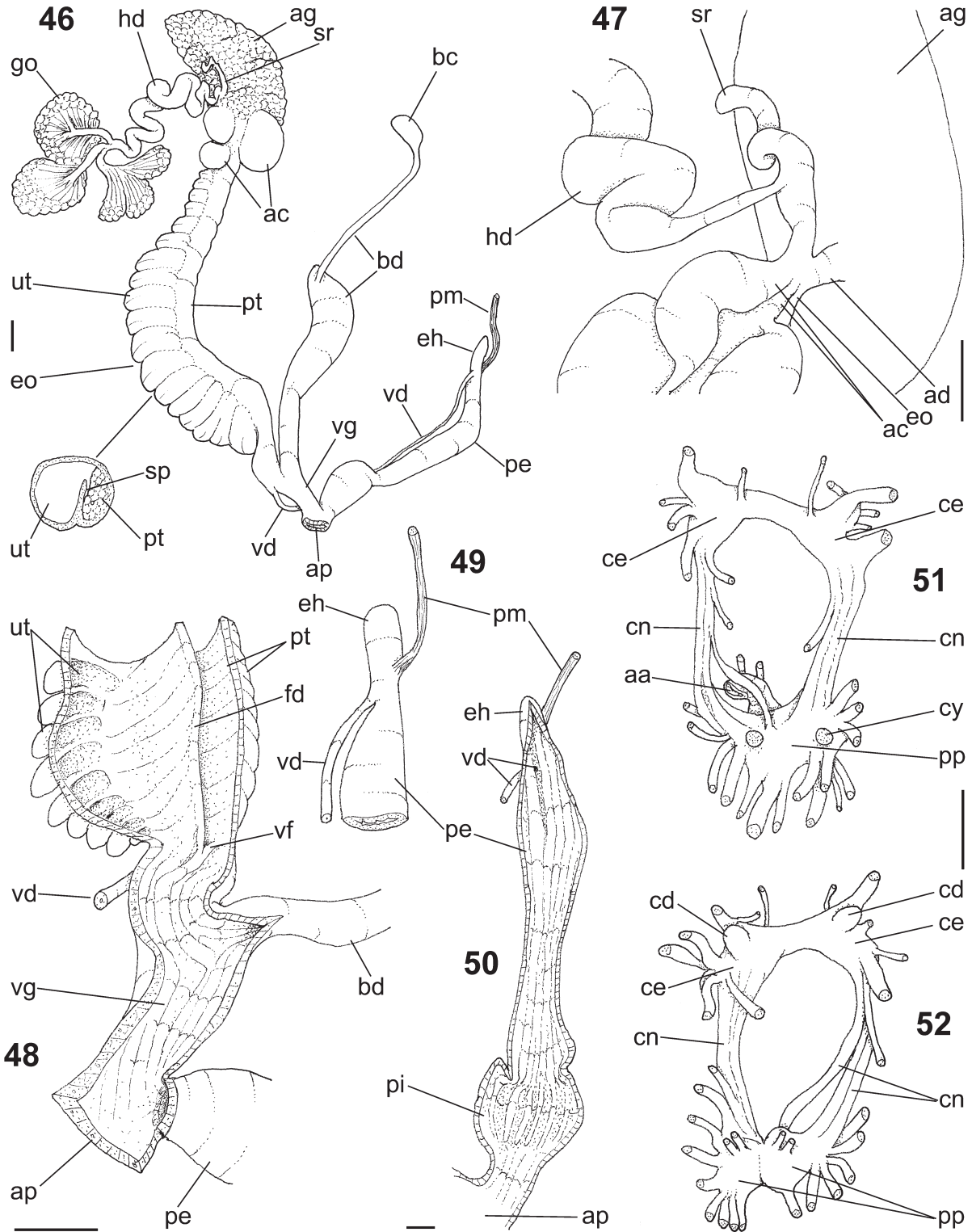
Genital system (Figs. 46–50): features similar to *Leiostracus carnavalescus* (see above), with the following differences: Gonad with more distinct lobes (Fig. 46: go). Hermaphroditic duct shorter, less coiled and much thicker (Figs. 38, 46: hd). Insertion of hermaphroditic duct very narrow (Fig. 47: hd). Seminal receptacle narrower, coiled, ~10 times longer than wide (Fig. 47: sr). Fertilization complex about as wide as seminal receptacle and ~1/2 its length; anterior end of complex with wide albumen gland duct and pair of albumen chamber ducts on opposite side (Fig. 47: ad, ac). Albumen chambers (Figs. 46–47: ac) each of ~1/6 albumen gland size; the most posteriorly located chamber is duplicated. Spermoviduct slightly shorter and broader, of ~1 whorl in length, ~12 times longer than wide. Prostate gland occupying ~1/3 of spermoviduct volume (Fig. 46: pt). Uterus occupying other 2/3 of spermoviduct space; external walls with strong transverse folds (Fig. 46: ut); no posterior diverticulum (Fig. 47). Sperm groove is a tall fold on almost the entirety its length (Figs. 46, 48: fd); vas deferens exteriorization simple, connected to internal fold (Fig. 48: vf). Bursa copulatrix as long as spermoviduct; bursa duct as wide as adjacent spermoviduct near its origin, but gradually narrowing towards posterior end (Figs. 46, 48: bd), up to ~1/5 spermoviduct width; bursa with ~1/5 of albumen gland size (Fig. 46: bc); one specimen with bulging due to fusiform, elongated spermatophore (Fig. 46: bd). Penis ~1/2 spermoviduct length (Figs. 38, 46: pe); penis muscle short, inserting



Figs. 32–38. *Rhinus botocodus* n. sp., anatomy. **32.** Pallial cavity, in inner ventral view (ventral flap of pneumostome [pv] deflected). **33.** Mantle border, in frontal view (as in situ). **34.** Detail of pneumostome region, in ventral view (ventral flap of pneumostome [pv] deflected upwards). **35.** Posterior region of pallial cavity, in inner ventral view (heart and reno-pericardial apertures seen by transparency). **36.** Transverse section of the middle level of kidney (ventral side to the right). **37.** Head-foot, in dorsal view (most of the dorsal side of haemocoel removed to show columellar muscle components). **38.** Head-foot and visceral mass, mostly in ventral view (dorsal wall of haemocoel removed; pallial cavity partially shown; most structures seen as in situ). – Scale bars: 2 mm.



Figs. 39–45. *Rhinus botocodus* n. sp., anatomy. – **39.** Foregut and midgut, in dorsal view (some adjacent structures are also shown). **40.** Buccal mass, in ventral view (odontophore partially removed and deflected to the right). **41.** Buccal mass, in lateral (right) view. **42.** Odontophore, in ventral view (right intrinsic muscles deflected; part of subradular membrane [br] removed on the right side). **43.** Odontophore, in dorsal view (radula still partially connected, but deflected downwards). **44.** Right odontophore cartilage, in dorsal view, showing origin of the intrinsic muscles. **45.** Right odontophore cartilage, in ventral view. – Scale bars: 2 mm.



Figs. 46–52. *Rhinus botocudus* n. sp., anatomy. – 46. Genital system, in ventral view (with cross-section of indicated portion of spermoviduct). 47. Genital system, detail of region of carrefour (albumen gland [ag] seen as transparent structure). 48. Terminal region of genital system, in dorsal view (most of the female portion opened longitudinally). 49. Penis, detail of distal region. 50. Penis, in dorsal view, entirely opened longitudinally. 51. Central nervous system (nerve ring), in ventral view. 52. Central nervous system (nerve ring), in dorsal view. – Scale bars: 1 mm.

subterminally (Figs. 49–50: pm). Epiphallus is a simple blind sac, $\sim \frac{1}{8}$ penis length (Figs. 49–50: eh). Vas deferens inserted between epiphallus and penis (Figs. 49–50: vd). Internal penial surface lacking clear inner divisions, except for anterior wide short region (Fig. 50: pi); 5–6 longitudinal simple wide folds, closely packed together, but gradually becoming narrower and more distanced from each other towards anterior chamber (Fig. 50). Penis shield absent.

Central nervous system (Figs. 51, 52): features similar to *Leiostracus carnavalescus* (see above), with the following differences: Central nervous system located more anteriorly, mostly on the ventral base of buccal mass (Fig. 39: nr). Ganglia more separated and more individualized. Pair of cerebral ganglia (ce) more separated from each other; cerebral commissure about as long as each ganglion; each ganglion with about half the size of adjacent esophageal section. Between cerebral ganglia and pedal ganglia, there are three parallel symmetrical connectives (cn), each circa three times as long as cerebral ganglia. Pair of pedal ganglia (pp) forming single mass, about as large as cerebral ganglia; weak constriction between the two pedal ganglia. Statocysts with several iridescent internal granules (Fig. 51: cy). Buccal ganglia well-developed, located laterally between esophageal origin and odontophore (Fig. 40: bg).

Measurements (in mm). Holotype: 4.75 whorls; H = 13.9; D = 11.7; S = 5.6; S' = 3.4; h = 8.7; d = 7.6. Mean (n = 9): ~ 4.5 whorls; H = 14.7 ± 0.8 (max 15.9; min 13.9); D = 11.5 ± 0.6 (max 12.3; min 10.4); S = 6.0 ± 0.3 (max 6.4; min 5.4); S' = 3.5 ± 0.3 (max 3.8; min 2.9); h = 9.2 ± 0.5 (max 10.1; min 8.4); d = 7.4 ± 0.5 (max 8.2; min 6.6).

Distribution

Known only from type locality.

Habitat

Found on low foliage.

Remarks

Rhinus botocodus n. sp. is reminiscent of only two Brazilian species: *R. velutinohispidus* (Moricand, 1836) and *R. longisetus* (Moricand, 1846), both from Bahia state (SIMONE 2006). *Rhinus botocodus* can be distinguished from *R. velutinohispidus* by being much smaller, barely reaching half the size of that species, and having a deeper suture and more convex whorls. *Rhinus botocodus* can be distinguished from *R. longisetus* by being larger, having a narrower spire and a more laterally positioned body whorl. Finally, *R. botocodus* has an arrangement of hairs on the periostracum similar to *R. ciliatus* (Gould, 1846), from Rio de Janeiro state (SIMONE 2006); nevertheless, it can be differentiated from this species by its smaller size, more rounded shell profile, lower spire, a whitish band on the

middle portion of the body whorl and more separate spiral lines of hair.

Rhinus is an endemic South American genus, occurring in Venezuela and Brazil, being particularly diverse in the latter (BREURE 1979, SIMONE 2006). Anatomically, the distinctive description above explored the main exclusivities of *R. botocodus* when compared with the known orthalicoids, and with *Leiostracus carnavalescus* described above. Particularly, the more remarkable exclusivities are: the origin of the tentacular muscle in the columellar muscle (Fig. 37); the absence of the esophageal duct to the anterior lobe of the digestive gland, which instead is located in the stomach (Fig. 39); the presence of three albumen chambers (Fig. 46); and the simple internal surface of the penis (Fig. 50). Additionally, of great interest are the multiple columellar muscles (Fig. 37: cm), similar to what is seen in *Leiostracus carnavalescus*. The analysis of these differences and shared features is still a matter of ongoing analysis.

Family Subulinidae Genus *Obeliscus* Beck, 1837

Obeliscus boitata n. sp. (Figs. 77–79)

Type material

Holotype: MZSP 106169 (Figs. 77–79).

Paratypes: MZSP 106170 (39 shells), from type locality. J. COLTRO col., May/2012.

Type locality: Brazil. Minas Gerais: Nanuque, ~ 120 m of elevation ($\sim 17^{\circ}51'S$ $40^{\circ}23'W$).

Etymology

The name (in apposition) is a reference to Boitatá, a fiery snake-like creature that protected the forests in Brazilian folklore.

Distribution

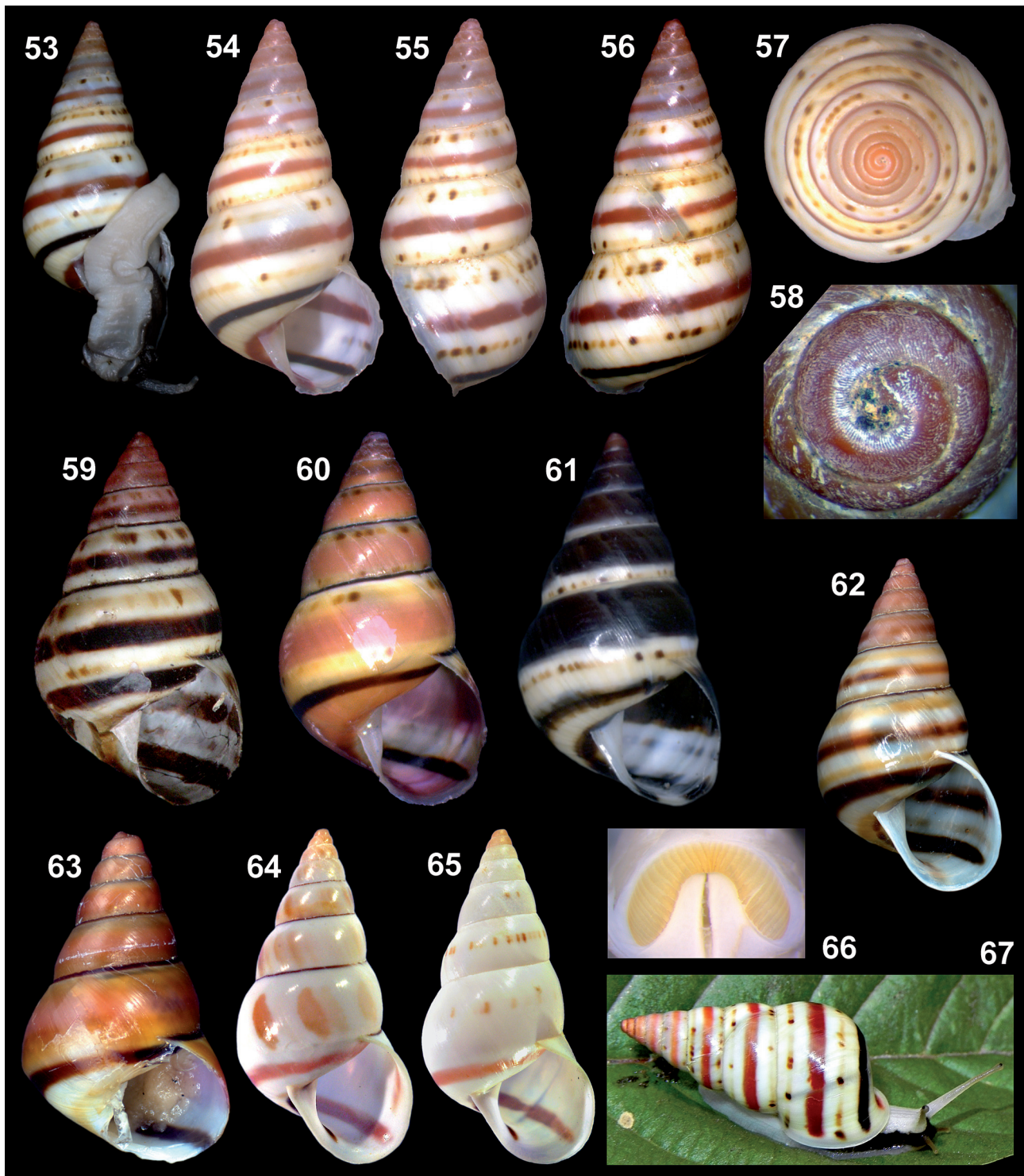
Known only from type locality.

Diagnosis

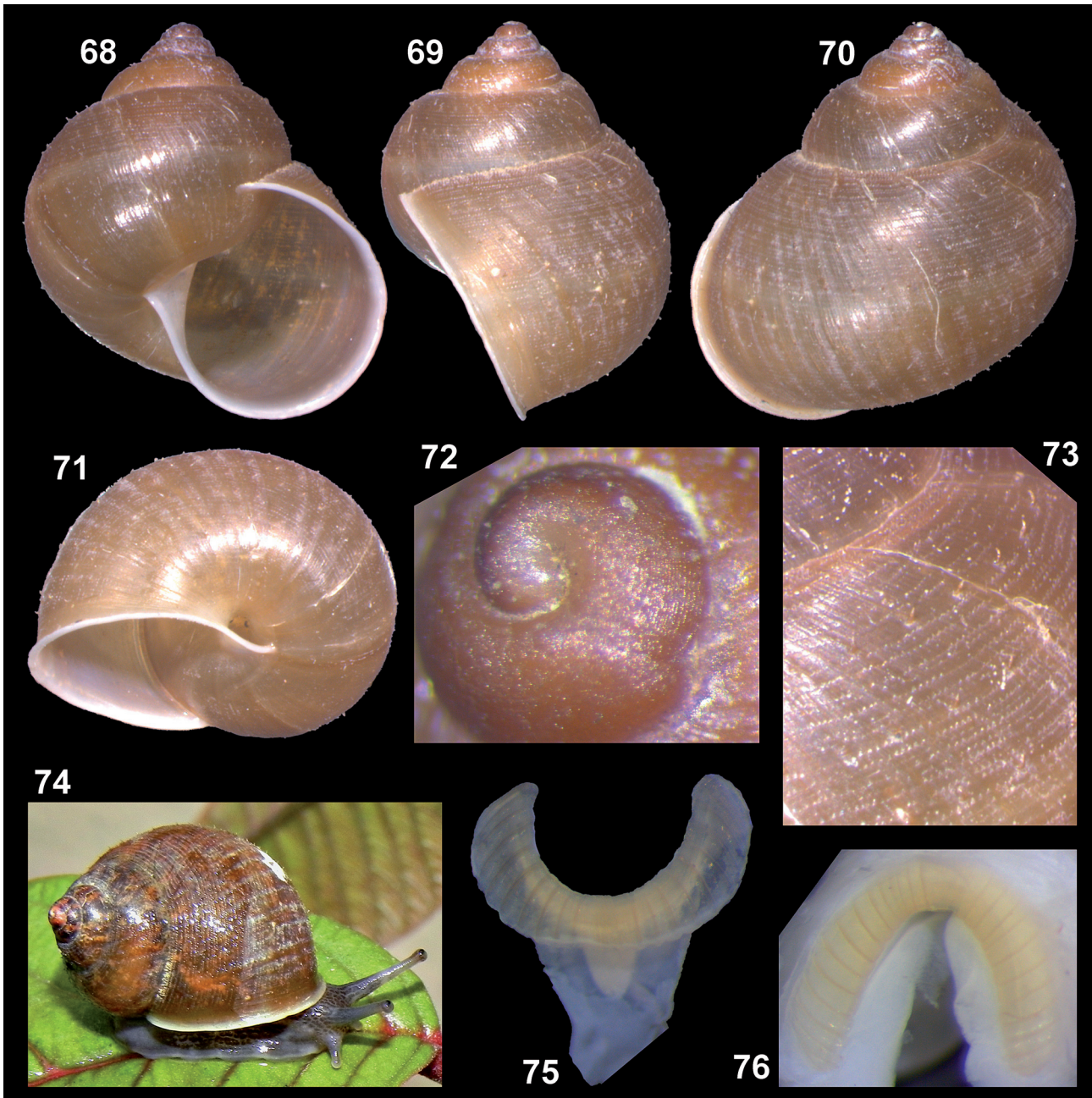
Spire top narrow, elongated. Spire apex (protoconch) bulbous, domed, thicker than subsequent spire portion. Suture perpendicular to shell length axis. Whorls with a faint keel on median region. Aperture rectangular.

Description

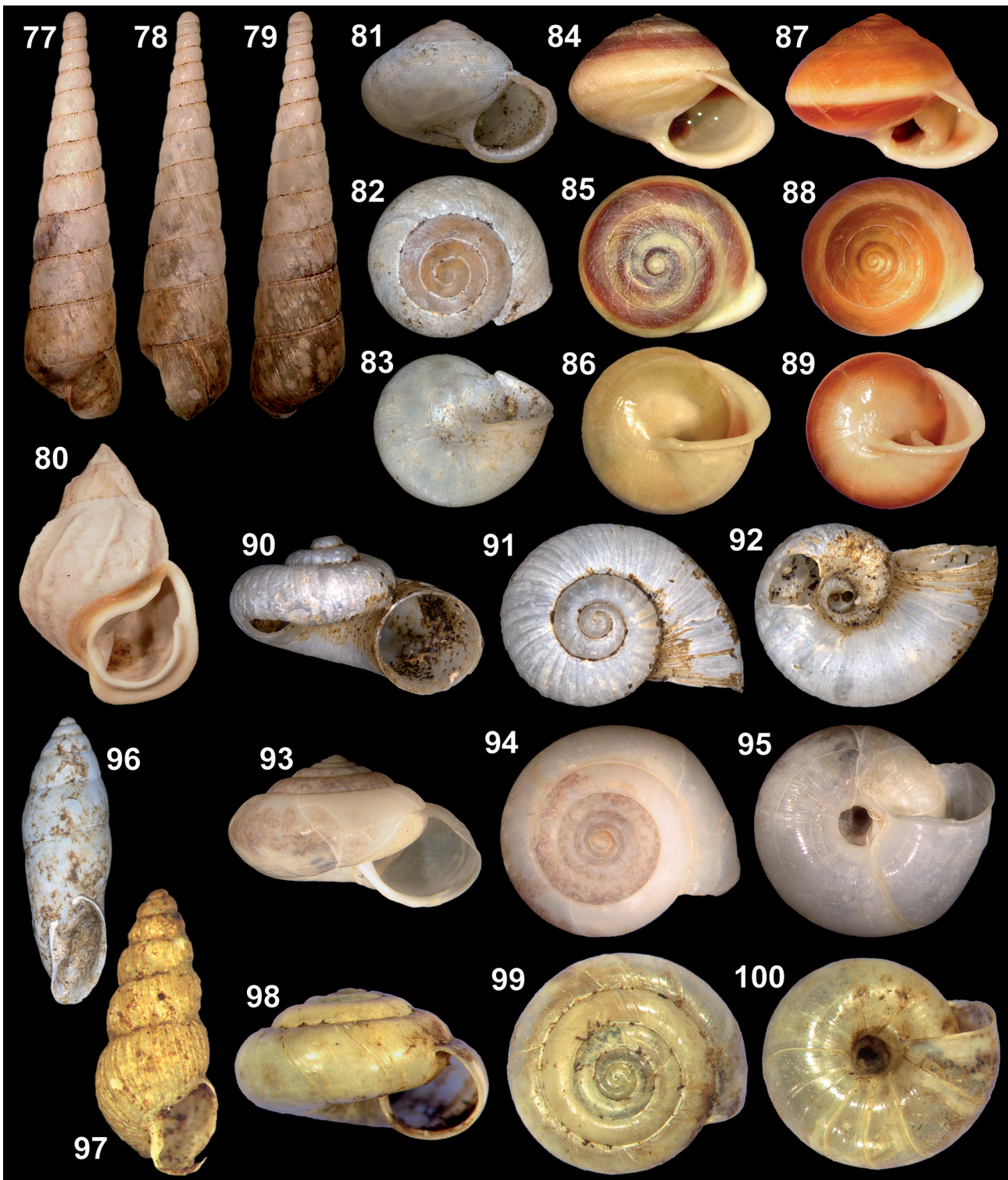
Shell large, multispiral, thin, conical, imperforate; spire top narrow, elongated. Spire apex (protoconch) bulbous, domed, thicker than subsequent spire portion; diameter $\sim \frac{1}{4}$ shell length. Color translucent white to dirty white. Spire angle $\sim 15^{\circ}$. Protoconch of ~ 2.75 whorls, rounded, dome-shaped, blunt, smooth; transition



Figs. 53–67. *Leiostracus carnavalescus* n. sp. – 53–57. Holotype (MZSP 106177; H=25.4 mm). 58. Holotype, protoconch detail (inferior side = 2 mm). 59. Paratype #1 (MZSP 106179). 60. Paratype #2 (MZSP 106178; H=21.2 mm). 61. Paratype #3 (MZSP 106179). 62. Specimen #1 from Pinheiros, Espírito Santo (MZSP 106618; H=21.2 mm). 63. Specimen #2 (juvenile) from Sooretama, Espírito Santo (MZSP 106666; H=10.3 mm). 64. Specimen #1 from Mantena, Minas Gerais (MZSP 108010). 65. Specimen #2 from Mantena, Minas Gerais (MZSP 108010). 66. Detail of mouth showing exposed portion of jaw (inferior side = 3 mm). 67. Living specimen, paratype #4 (MZSP 106178).



Figs. 68–76. *Rhinus botocodus* n. sp. – 68–71. Holotype (MZSP 106174; H = 13.9 mm, D = 11.7 mm). 72. Same, detail of shell apex (inferior side = 2 mm). 73. Same, detail of surface in middle-right side of last whorl, showing hairy periostracum (right side = 3 mm). 74. Living specimen, paratype (MZSP 106175, H = 15.3 mm). 75. Extracted jaw, in anterior to slightly posterior view (width = 1.2 mm). 76. Jaw, as seen in situ, in anterior view.



Figs. 77–100. Land snails from Nanuque, Minas Gerais State, Brazil. – 77–79. *Obeliscus boitata* n. sp., holotype (MZSP 106169; H = 50.3 mm). 80. *Auris bilabiata* (MZSP 106155; H = 42 mm). 81–83. *Helicina boettgeri* (MZSP 106166; D = 4.1 mm). 84–86. *Helicina variabilis*, specimen #1 (MZSP 106171; D = 12.9 mm). 87–89. *Helicina variabilis*, specimen #2 (MZSP 106172; D = 12.5 mm). 90–92. *Cyclopomops moricandi* (MZSP 106168; D = 5.1 mm). 93–95. *Rectartemon piquetensis* (MZSP 106156; D = 31.6 mm). 96. *Bahiensis* cf. *bahiensis* (MZSP 106165; H = 16.2 mm). 97. *Dysopeas muibum* (MZSP 106163; H = 5.7 mm). 98–100. *Prohappia besckei* (MZSP 106164; D = 7.1 mm).

to teleoconch clear. Teleoconch sculptured by numerous thin axial striae, stronger on the upper portion of whorl near the suture. Whorl profile slightly convex; faint keel on median region. Suture well-marked. Aperture small, prosocline, oval to rectangular; $\sim 1/5$ shell length, $\sim 1/2$ shell width. Peristome simple, weakly reflexed. Body whorl $\sim 1/4$ shell length.

Measurements (in mm). Holotype: 13.75 whorls; H = 50.3; D = 11.9; S = 40.9; S' = 35.9; h = 9.7; d = 6.1. Mean (n = 10): from 13.5 to 14.5 whorls; H = 49.1 \pm 1.9 (max 52.0; min 47.0); D = 11.5 \pm 0.4 (max 11.9; min 10.8); S = 40.1 \pm 1.8 (max 43.2; min 38.0); S' = 35.6 \pm 1.3 (max 37.9; min 33.7); h = 9.4 \pm 0.4 (max 10.0; min 8.6); d = 6.0 \pm 0.3 (max 6.4; min 5.6).

Remarks

Obeliscus boitata n. sp. closely resembles, in overall shell shape and color, only *O. carphodes* (Pfeiffer, 1852) and *O. sylvaticus* (Wagner, 1827); the known distribution of the latter is given as a vague “northeastern Brazil”, while the former’s is even vaguer, given simply as “Brazil” (SIMONE 2006). *Obeliscus boitata* n. sp. can be distinguished from both these species by its narrow and elongated spire, bulbous protoconch, faint keel and a suture more perpendicular to the shell length’s axis. It can be further differentiated from *O. carphodes* by its smaller size and rectangular aperture and from *O. sylvaticus* by its larger size and shorter whorls.

4 Discussion

Besides the new species described above, a list of the other species found in the land snail sample from Nanuque can be seen on Tab. 1. The records of some species presented here are the first ones for Minas Gerais state: *Auris bilabiata* (Broderip & Sowerby, 1829) (Fig. 80), *Helicina boettgeri* Wagner, 1910 (Figs. 81–83), *Helicina variabilis* Wagner, 1827 (Figs. 84–89), *Cyclopomops moricandi* (Pfeiffer, 1852) (Figs. 90–92), *Rectartemon piquetensis* (Pilsbry, 1930) (Figs. 93–95), *Bahiensis* cf. *bahiensis* (Moricand, 1833) (Fig. 96), *Dysopeas muibum* Marcus & Marcus, 1968 (Fig. 97) and *Prohappia besckei* (Dunker in Pfeiffer, 1847) (Figs. 98–100). Although Nanuque is located very close to the borders with Bahia and Espírito Santo states (Fig. 1), the present records still represent an extension in the distribution of these species (Tab. 1). Most of the species presented here belong to genera already well recorded for the Brazilian southeast region, but three genera in particular (*Cyclopomops* Bartsch & Morrison, 1942, *Dysopeas* Baker, 1927 and *Prohappia* Thiele, 1927) are completely new records for Minas Gerais.

The natural environment around Nanuque was severely degraded by incessant woodcutting, crops, breeding of livestock and the construction of railroads

and highways since the final decades of the 19th century (CERQUEIRA NETO 2005, MARTINS 2010). Nevertheless, the single forest fragment studied here still harbors a unique fauna and even new species. Our findings in Nanuque are a reminder of how these remnants of Atlantic rainforest might be acting as refuges (e. g., PEREIRA et al. 2014), harboring still unknown diversity and perhaps even their own share of endemic species. Despite the regions’ flora and fauna being scarcely studied, a high level of biodiversity is thought to be the norm for the broader region encompassing Nanuque and its surroundings and concerns about extinction have already been raised for plant and fish species (CERQUEIRA NETO 2005, SARMENTO-SOARES et al. 2007).

Alarmingly, JOSÉ COLTRO Jr. and his team returned much more recently to the same forest fragment in Nanuque, only to discover that it was nearly entirely devastated in order to open space for more tomato crops. Whether the new species described here have already become extinct remains to be seen, as they may still live unknown and undisturbed in other localities (*Leiostracus carnavalescus*, for instance, also occurs elsewhere). Still, it is well-known that many species are becoming extinct before been even known to science (e. g., HAWKSWORTH & COWIE 2013), even in groups prone to greater study and protection efforts, like birds (e. g., PEREIRA et al. 2014). Therefore, the situation might be much direr for land and freshwater mollusks, which are deemed the most imperiled group of animals, with the highest extinction rates (LYDEARD et al. 2004, RÉGNIER et al. 2008). Despite basic science being currently out of vogue, a more thorough knowledge of the local fauna and flora of these critical places is the first step towards protection and appropriate legislation.

5 References

- BREURE, A. S. H. (1979): Systematics, phylogeny and zoogeography of Bulimulinae (Mollusca). – Zoologische Verhandelingen **168**: 1–215.
- BREURE, A. S. H. & SCHOUTEN, J. R. (1985): Notes on and descriptions of Bulimulidae (Mollusca, Gastropoda), III. – Zoologische Verhandelingen **216**: 1–98.
- CERQUEIRA NETO, S. P. G. (2005): Contribuição ao estudo geográfico do município de Nanuque (MG). – Caminhos de Geografia **9** (15): 82–92.
- HAWKSWORTH, D. L. & COWIE, R. H. (2013): The discovery of historically extinct, but hitherto undescribed, species: an under-appreciated element in extinction-rate assessments. – Biodiversity and Conservation **22**: 2429–2432.
- LYDEARD, C., COWIE, R. H., PONDER, W. F., BOGAN, A. E., BOUCHET, P., CLARK, S. A., CUMMINGS, K. S., FREST, T. J., GARGOMINY, O., HERBERT, D. G., HERSHLER, R., PEREZ, K. E., ROTH, B., SEDDON, M., STRONG, E. E. & THOMPSON, F. G. (2004): The Global Decline of Nonmarine Mollusks. – BioScience **54**: 321–330.
- MARTINS, M. L. (2010): Ocupação e desflorestamento numa área de fronteira: Vale do Mucuri, MG: 1890 a 1950. – Revista de História Regional **15**: 40–77.

- MORRETES, F. L. (1949): Ensaio de catálogo dos moluscos do Brasil. – Arquivos do Museu Paranaense 7: 5–216.
- PEREIRA, G. A., DANTAS, S. M., SILVEIRA, L. F., RODA, S. A., ALBANO, C., SONNTAG, F. A., LEAL, S., PERIQUITO, M. C., MALACCO, G. B. & LEES, A. C. (2014): Status of the globally threatened forest birds of northeast Brazil. – Papéis Avulsos de Zoologia 54 (14): 177–194.
- RÉGNIER, C., FONTAINE, B. & BOUCHET, P. (2008): Not knowing, not recording, not listing: numerous unnoticed mollusk extinctions. – Conservation Biology 23: 1214–1221.
- ROBINSON, D. G. & SLAPCINSKY, J. (2005): Recent introductions of alien land snails into North America. – American Malacological Bulletin 20: 89–93.
- SALVADOR, R. B. & CAVALLARI, D. C. (2013): Taxonomic revision of *Leiostracus onager* and *Leiostracus subtuszonatus* (Gastropoda: Pulmonata: Orthalicidae). – Journal of Conchology 41: 511–518.
- SARMENTO-SOARES, L. M., MAZZONI, R. & MARTINS-PINHEIRO, R. F. (2007): A fauna de peixes na bacia do Rio Peruípe, extremo Sul da Bahia. – Biota Neotropica 7: 291–308.
- SIMONE, L. R. L. (1998): Anatomical description of *Anctus angustomus* (Wagner, 1827) from northeastern Bahia, Brazil (Gastropoda, Pulmonata, Bulimulidae). – Studies on Neotropical Fauna and Environment 33: 170–177.
- SIMONE, L. R. L. (2006): Land and freshwater mollusks of Brazil, 390 pp.; São Paulo (Editora Gráfica Bernardi & Fundação de Amparo à Pesquisa do Estado de São Paulo).

Authors' addresses:

LUIZ RICARDO LOPES SIMONE, Museu de Zoologia da Universidade de São Paulo, Avenida Nazaré 481, 04218-970 São Paulo, Brazil; e-mail: lrsimone@usp.br

RODRIGO BRINCALEPE SALVADOR (corresponding author), Staatliches Museum für Naturkunde Stuttgart, Rosenstein 1, 70191, Stuttgart, Germany or Mathematisch-Naturwissenschaftliche Fakultät, Eberhard Karls Universität Tübingen, Hölderlinstraße 12, 72074 Tübingen, Germany; e-mail: salvador.rodrigo.b@gmail.com

Manuscript received: 22.IX.2015, accepted: 25.XI.2015.